ChemComm

Cite this: *Chem. Commun.*, 2011, **47**, 5157–5159

www.rsc.org/chemcomm

COMMUNICATION

A new route for the synthesis of polyhedral gold mesocages and shape effect in single-particle surface-enhanced Raman spectroscopy†

Jixiang Fang,*[ab] Sergei Lebedkin,[b] Shengchun Yang*[a] and Horst Hahn[b]

Received 18th January 2011, Accepted 1st March 2011
DOI: 10.1039/c1cc10328h

We have demonstrated a new strategy to synthesize Au mesocages using polyhedral Cu_2O templates. The obtained polyhedral Au mesocages show a strong shape effect in highly sensitive single-particle surface-enhanced Raman spectroscopy (sp-SERS).

SERS-based signal detection and molecular identification is a powerful chemical sensing method with numerous potential applications in biomedicine, life science, analytical chemistry, *etc*.[1] "Hot spots" where a local Raman enhancement is as high as $\sim 10^{10}$ or more have been observed for a number of substrates and nanoparticle aggregates by using Raman microscopy techniques.[1b] However, the lack of reproducibility and reliability with high sensitivity still hampers practical applications of SERS molecule detection.

For some applications, just one micro- or nanoparticle can be envisaged as a sp-SERS sensor combining a high sensitivity with a high spatial resolution, for example, recent reports about novel gold and silver mesoscale particles or mesostructures.[2] These particles demonstrate a highly roughened surface with irregular nanoscale protrusions and crevices. Such surface topography makes these nanoparticles very attractive for many plasmonic-based applications, including sp-SERS sensors.

Noble metal nanocages represent a class of nanostructures with high specific surface areas, low densities, hollow interiors and porous walls. They display particular surface plasmon resonance (SPR) properties (manifested, *e.g.*, in a red shift of the extinction resonances relative to colloids of "solid" Au nanoparticles). Previous studies have indicated that gold nanocages and nanoshells can also exhibit a very high SERS enhancement depending on their size, shape, surface roughness, and the geometry of the shell and core (or interior cavity).[3] Up to now, gold nanocages have been intensively synthesized by Xia and by several other groups using silver cubes or Co nanospheres as sacrificial templates *via* the galvanic replacement method.[4] However, with these templates, it was difficult to synthesize more diverse hollow noble metal nanostructures. For example, due to non-sophisticated templates up to now, the reports of more active metal or alloy nanocages, *e.g.*, silver nanocages, were quite few, particularly for the polyhedral nanocages owing to no polyhedral templates being available.

Here, we report a new strategy to synthesize polyhedral Au hollow mesostructures using Cu_2O as templates. We investigate the shape effect-dependent SERS activity of the product obtained by the current template route. The produced polyhedral gold mesocages possess unique structural features such as highly roughened surface topography and exhibit a remarkably high SERS activity, making them very appealing as sp-SERS sensors. Importantly, polyhedral gold mesocages consist of a great number of nanoparticle building units hereinto include an abundant amount of effective hot spots in the vicinity of the corrugated and creviced regions between these nanoparticles. This highly repeatable intraparticle structure (intraparticle interaction) results in a highly repeatable and reproducible SERS signal. One of the advantages is that a variety of shapes of Cu_2O templates have been reported so far,[5] which can be easily accessed and applied in the replacement reaction protocol. Additionally, the current synthetic protocol would be also employed to obtain various components such as, Ag, Au, Pt, Pd and their alloys.

The replacement reaction of our synthetic protocol was described in ESI† and schematically shown in Fig. S1 (ESI†). Fig. 1a and c–e present typical SEM and TEM images of the cubic Cu_2O synthesized by reducing a copper sulfate solution with glucose in the presence of PVP. The sizes of the cubes typically range within a narrow size distribution from 500 to 600 nm (Fig. 1c). The TEM image (Fig. 1d) and the corresponding SAED pattern (Fig. 1e) reveal that they are single crystals. By the reaction of these Cu_2O polyhedrons with $HAuCl_4$ aqueous solution, gold mesocages with uniform morphology similar to that of the Cu_2O template are obtained. The gold cubes (Fig. 1b) show a very rough surface with small nanoparticles aggregated. The TEM image of the gold cubic nanocages (Fig. 1f) demonstrates a clear hollow interior and thin walls. A strong contrast difference between the edges (dark) and center (bright) in Fig. 1f implies that the cubic nanocages have a wall thickness of around tens of nanometres. The SAED patterns recorded from single gold cubic nanocages (Fig. 1g) reveal the typical polycrystalline nature of the obtained cubic gold nanocages.

[a] *School of Science, MOE Key Laboratory for Nonequilibrium Synthesis and Modulation of Condensed Matter, Xi'an Jiaotong University, Shann Xi, 710049, People's Republic of China. E-mail: jxfang@mail.xjtu.edu.cn, ysch1209@mail.xjtu.edu.cn; Tel: +86 29-52665995*
[b] *Karlsruhe Institut für Technologie (KIT), Institut für Nanotechnologie, Karlsruhe 76021, Germany*

† Electronic supplementary information (ESI) available: UV-vis absorption spectra, SEM images and EDX pattern. See DOI: 10.1039/c1cc10328h

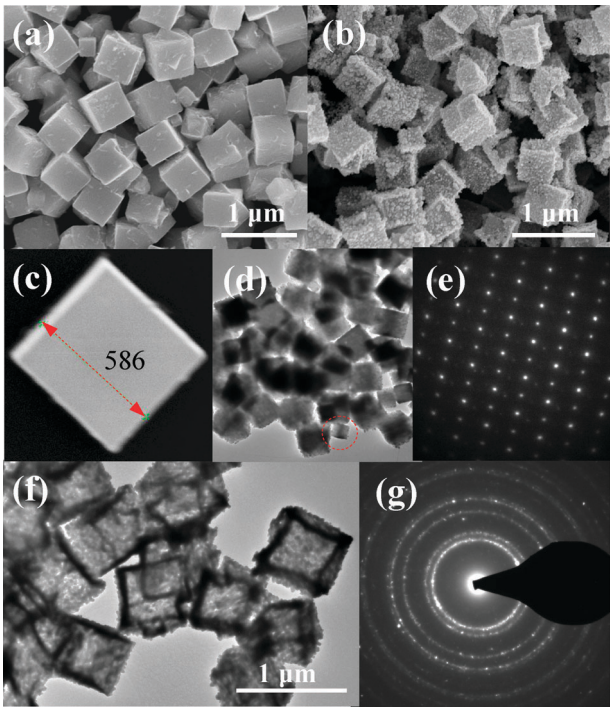

Fig. 1 SEM and TEM images of cubic Cu_2O and gold mesocages. (a) and (c) SEM images of Cu_2O cubes. (d) and (e) TEM image and SAED pattern of Cu_2O cubes recorded from the cycle area in Fig. 2d. (b) SEM image of Au cubic mesocages. (f) and (g) TEM images of Au cubic mesocages and the SAED pattern obtained from a whole Au cubic mesocage.

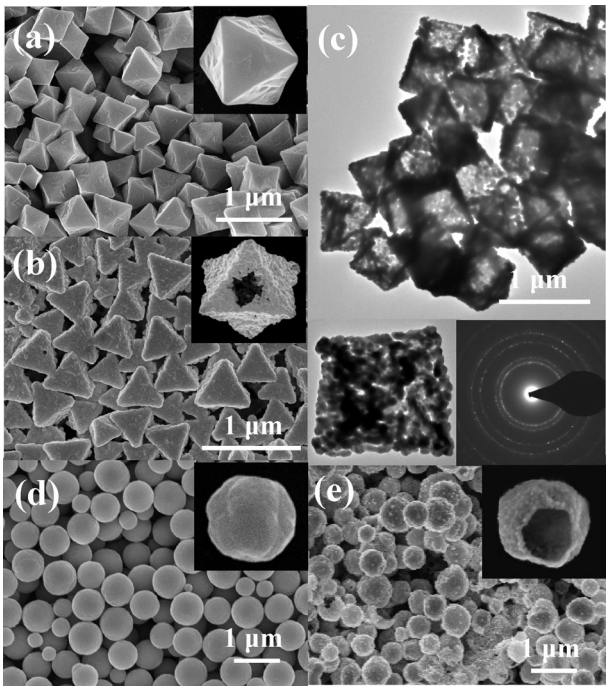

Fig. 2 (a) SEM image of Cu_2O octahedrons, inset showing the magnified image. (b) and (c) SEM and TEM images of Au octahedral mesocages. Insets show the magnified images and the SAED pattern obtained from single Au mesooctahedron. (d) SEM image of Cu_2O spheres, inset showing the magnified sphere. (e) SEM images of spherical Au mesocages. Inset shows the magnified broken Au mesosphere.

Similar to the formation of cubic Cu_2O nanostructures, by adjusting the PVP concentrations in the reaction solution, octahedral and spherical Cu_2O templates have also been produced as shown in Fig. 2a and d. The sizes of the Cu_2O octahedrons and spheres typically are around 600 nm and 800 nm, respectively. The insets of Fig. 2a and d clearly display the morphology of the Cu_2O octahedrons and spheres. By the reaction of these Cu_2O polyhedrons with $HAuCl_4$ solution, octahedral and spherical gold nanocages have also been synthesized with the main edge lengths of 600–700 nm for the former and 800–900 nm for the latter. The insets of Fig. 2b and e show the morphology of the incomplete hollow gold nanocages. The corresponding TEM images (Fig. 2c) clearly display a hollow interior and a rough surface. The SAED patterns recorded from single gold octahedron reveal the typical polycrystalline nature of the obtained polyhedral gold nanocages.

In order to extend the possibility of Cu_2O templates in synthesizing hollow nanostructures for various metals or alloy systems, we also prepare Ag and PtAu nanocages, using polyhedral Cu_2O templates. Fig. S2 and S3 (ESI†) show the typical morphologies for cubic Ag nanocages and octahedral PtAu nanocages by means of the similar reduction processes as gold polyhedral nanocages. The EDX spectra in Fig. S2 and S3 (ESI†) indicate that a few amount of residual Cu can be observed. It is noted that Cu_2O templates demonstrate a very robust capacity of synthesizing nanostructures for a variety of materials, *e.g.*, the quite few reported Ag nanocages. Such nanostructures may find important applications in various areas of catalysis, biology, optics, *etc.*

The investigation of the polyhedral gold mesocages with regard to their sp-SERS activity was performed by using crystal violet (CV) dye. Two types of the Raman experiments were performed. By the first one, SERS signal distributions across individual nanocages were characterized (mapped) with a high spatial resolution of $\sim$0.4 μm (100×, NA = 0.9) and the confocal mode of the microscope. Fig. 3 (left column) shows typical sp-SERS images of polyhedral gold mesocages as well as a gold nanoparticle of a similar size ($\sim$400 nm) synthesized for comparison (see Fig. S4, ESI†). The color code in Fig. 3 represents the intensity of a strong Raman band of CV at 1172 cm^{-1} integrated over 1120–1250 cm^{-1}. From comparison of the maximal signals observed (numbers on top of the color-code scale bars), the SERS activity was found to increase in a series: gold nanoparticle < spherical nanocage ≪ cubic nanocage < octahedral nanocage. Moreover, the SERS images were found to be quite uniform over their entire surface as illustrated in Fig. 3c and d, implying multiple, similarly active "hot spots" homogeneously distributed over the cubic and octahedral nanocages—an advantageous feature for the spSERS sensor.

By the second type of Raman measurements, the SERS spectra "averaged" over individual particles were acquired. A particle was visually centered within the laser excitation/emission collection spot of $\sim$3 μm (20×). Fig. 3 (right column) shows spSERS spectra obtained in this way for individual gold nanoparticles and nanocages. The spectra demonstrate three strong peaks at 1172, 1371 and 1619 cm^{-1} and are well consistent with the normal Raman spectrum of CV.

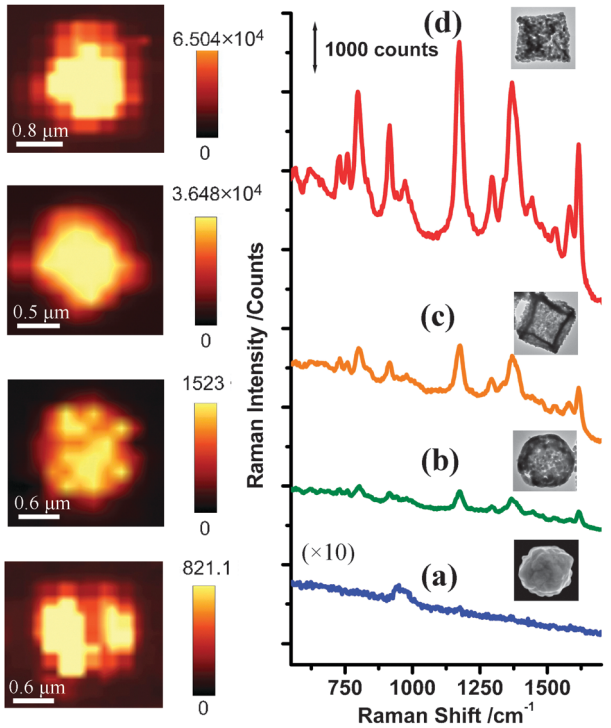

Fig. 3 Single-particle SERS spectra and images of crystal violet (CV) on a gold nanoparticle (a) and gold nanocages with (b) spherical, (c) cubic, and (d) octahedral shapes. The spectra were acquired from individual nanostructures on Si substrates under the same conditions (20 s integration time and 0.1 mW excitation power at 633 nm excitation). The insets show typical SEM images of the corresponding particles.

Similar to the mapping results, the highest SERS signals were observed for the octahedral gold nanocages, up to $\sim 10^3$ higher than the signals from the gold nanoparticles. The SERS activity of the cubic nanocages was by a factor 4 lower as compared to the octahedral cages. Previous experiments and calculations suggest that the optimal SERS excitation wavelength for particles with a rough surface would lie in the red–near-infrared spectral region.[6] These may be further supported by UV-vis-NIR spectra which are shown in Fig. S5 (ESI†). As the shape of the gold polyhedral mesocages changing to more tips or corners, the localized surface plasmon bands appear in the red and infrared regions of the extinction spectrum. Importantly, the SERS signals from the cubic and octahedral cages were found to be remarkably reproducible within ±10% from one particle to another (more than 10 particles of each morphology were measured). We attribute the high SERS activity of the cubic and octahedral gold nanocages to their anisotropic architecture ("corner effect") and roughened surface.[7] In this regard, our observations are similar to a recent report on polyhedral silver nanoparticles, where the silver octahedron also manifested the highest SERS effect as compared with the silver cube and cuboctahedra.[8]

A SERS enhancement factor (EF) is a quantitative measure of the Raman signal amplification for a specific analyte. Following the procedure reported by Wang *et al.*[2a,9] and employing the CV peak at 1172 cm^{-1}, we estimated the EF of the polyhedral gold nanocages as about 2×10^7 and 5×10^6 for the octahedral and cubic gold nanocages, respectively (see details in ESI†). Taking into account the roughened surface of the nanocages, the above nanocage area may be underestimated and the EFs, consequently, overestimated. On the other hand, rinsing the substrates after CV deposition with water (see Experimental) can remove a significant fraction of CV molecules (assuming 1%–10% residual in ref. 9) and thus the EFs may be underestimated.

In conclusion, a new synthetic protocol using Cu_2O as sacrificial templates to form noble metal and alloy-polyhedral mesocages has been described. This strategy will open a new way to prepare hollow nanostructures for various metals and alloys. We found that the polyhedral gold mesocages, due to the highly roughened surface topography and anisotropic architecture, demonstrate a remarkably strong sp-SERS activity, *i.e.*, $\sim 10^7$–10^8 magnitude, for single mesoparticle. The SERS activity would be further improved by the aggregation or close-packed arrays of the resultant octahedral or cubic mesocages because of interparticle interactions generating additional "hot spots".[2] Importantly, the intraparticle interaction between the nanoparticle building units within the single mesoparticle creates multiple homogenously-distributed effective hot spots, herein, increases the reproducibility and reliability for the sp-SERS.

J. X. Fang thanks the support from "the National Basic Research Program of China (No. 2010CB635101)", the Tengfei Talent project of Xi'an Jiaotong University, "the Fundamental Research Funds for the Central Universities (No. 08142008), and "the National Natural Science Foundation of China (Nos. 50901056, 50834003)".

Notes and references

1 (*a*) J. F. Li, Y. F. Huang, Y. Ding, Z. L. Yang, S. B. Li, X. S. Zhou, F. R. Fan, W. Zhang, Z. Y. Zhou, D. Y. Wu, B. Ren, Z. L. Wang and Z. Q. Tian, *Nature*, 2010, **464**, 392; (*b*) M. S. Yavuz, Y. Y. Cheng, J. Y. Chen, C. M. Cobley, Q. Zhang, M. Rycenga, J. W. Xie, C. H. Kim, K. H. Song, A. G. Schwartz, L. H. V. Wang and Y. N. Xia, *Nat. Mater.*, 2009, **8**, 935; (*c*) I. A. Larmour, K. Faulds and D. Graham, *Chem. Sci.*, 2010, **1**, 151.

2 (*a*) J. X. Fang, S. Y. Du, Z. Y. Li, S. Lebedkin, R. Kruk and H. Hahn, *Nano Lett.*, 2010, **10**, 5006; (*b*) H. Wang and N. J. Halas, *Adv. Mater.*, 2008, **20**, 820; (*c*) H. Y. Liang, Z. P. Li, W. Z. Wang, Y. S. Wu and H. X. Xu, *Adv. Mater.*, 2009, **21**, 4614.

3 (*a*) M. Rycenga, Z. P. Wang, E. Gordon, C. M. Cobley, A. G. Schwartz, C. S. Lo and Y. N. Xia, *Angew. Chem., Int. Ed.*, 2009, **48**, 9924; (*b*) M. A. Ei-Sayed and M. A. Mahmoud, *Nano Lett.*, 2009, **9**, 3025.

4 (*a*) S. E. Skrabalak, J. Y. Chen, Y. G. Sun, X. M. Lu, L. Au, C. M. Cobley and Y. N. Xia, *Acc. Chem. Res.*, 2008, **41**, 1587; (*b*) H. P. Liang, L. J. Wan, C. L. Bai and L. Jiang, *J. Phys. Chem. B*, 2005, **109**, 7795.

5 K. X. Yao, X. M. Yin, T. H. Wang and H. C. Zeng, *J. Am. Chem. Soc.*, 2010, **132**, 6131.

6 (*a*) H. Wang, Y. P. Wu, B. Lassiter, C. L. Nehl, J. H. Hafner, P. Nordlander and N. J. Halas, *Proc. Natl. Acad. Sci. U. S. A.*, 2006, **103**, 10856; (*b*) H. Wang, G. P. Goodrich, F. Tam, C. Oubre, P. Nordlander and N. J. Halas, *J. Phys. Chem. B*, 2005, **109**, 11083.

7 (*a*) J. M. Mclellan, Z. Y. Li, A. R. Siekkinen and Y. N. Xia, *Nano Lett.*, 2007, **7**, 1013; (*b*) L. Rodriguez-Lorenzo, R. A. Alvarez-Puebla, I. Pastorize-Santos, S. Mazzucco, O. Stephan, M. Kociak, L. Liz-Marzan and F. J. G. Abajo, *J. Am. Chem. Soc.*, 2009, **131**, 4616.

8 M. Mulvihill, A. Tao, K. Benjauthrit, J. Arnold and P. D. Yang, *Angew. Chem., Int. Ed.*, 2008, **47**, 6456.

9 Y. Wang, M. Becker, L. Wang, J. Q. Liu, R. Scholz, J. Peng, U. Gosele, S. Christainsen, D. H. Kim and M. Steinhart, *Nano Lett.*, 2009, **9**, 2384.